Hindawi
Adsorption Science & Technology
Volume 2022, Article ID 2598536, 10 pages
https://doi.org/10.1155/2022/2598536

Research Article

A Facile Synthesis and Properties of Graphene Oxide-Titanium Dioxide-Iron Oxide as Fenton Catalyst

Bhawana Jain,[1] **Jaya V. Gade**,[2] **Arti Hadap**,[3] **Huma Ali**,[4] **Khadijah Mohammedsaleh Katubi**,[5] **Bashyam Sasikumar**,[6] **and Reena Rawat**[7]

[1]*Department of Chemistry, Govt. V.T.Y.PG. Autonomous College, Durg, 491001 Chhattisgarh, India*
[2]*Department of Analytical Chemistry, SNDT Women's University, Mumbai, 400049 Maharashtra, India*
[3]*Mukesh Patel School of Technology, Management & Engineering, NMIMS, Mumbai, India*
[4]*Department of Chemistry, Maulana Azad National Institute of Technology Bhopal, India*
[5]*Department of Chemistry, College of Science, Princess Nourah bint Abdulrahman University, P.O. Box 84428, Riyadh 11671, Saudi Arabia*
[6]*Faculty of Mechanical and Production Engineering, Arba Minch University, Arba Minch, Ethiopia*
[7]*Department of Chemistry, Echelon Institute of Technology, Faridabad, 121101 Haryana, India*

Correspondence should be addressed to Bhawana Jain; bhawanajain123@gmail.com
and Bashyam Sasikumar; bashyam.sasikumar@amu.edu.et

Received 20 January 2022; Revised 18 February 2022; Accepted 21 February 2022; Published 26 March 2022

Academic Editor: Adrián Bonilla-Petriciolet

Textile industries discharge wastewater in huge amount that contains several toxic contaminants, especially organic dyes. Organic dyes present in wastewater have many adverse effects on environment as well as on living organisms including human beings. The generation of a nanocomposite to trap the toxic organic dyes from wastewater is highly recommended. Herein, we report the preparation of graphene-iron-titanium oxide (GFT) nanocomposite using simple, practical, and cost-effective protocol. The prepared tri-nanocomposite was successfully recognized by employing several analytical techniques. Morphology of the prepared nanocomposites was assessed by SEM coupled with EDS (energy dispersive spectroscopy). HRTEM was used to measure the size of the nanocomposites with shape and morphology. The UV-visible absorption spectra of the nanocomposites were recorded by a UV-visible spectrophotometer. Finally, the crystal structures of the nanocomposites were confirmed by XRD. Moreover, we proposed a plausible mechanism to demonstrate the catalytic activity of GFT oxide nanocomposite for the degradation auramine (AM) dye via a heterogeneous Fenton process.

1. Introduction

Water is responsible for the origin of life on the planet earth as well as it is necessary too for the existence of all lives. Due to the prevalence of industrialization, urbanization, and population explosion, the natural water reservoirs have been contaminated by different types of heavy metals, pharmaceuticals, chlorinated hydrocarbons, and organic dyes [1–3]. Therefore, extensive efforts are highly desirable to protect natural water resources from pollutants as well as to supply clean water to living beings. In this context, to provide a healthy and safe future to our generations, numerous systematic strategies for removal of pollutants from wastewater were reported such as membrane filtration, coagulation, electrochemical treatments, chemical precipitation, solvent extraction, flotation, evaporation, adsorption, biosorption, reverse osmosis, and ion exchange [4–9]. Among the aforementioned strategies, adsorption is regarded as one of the most explored strategy for removing contaminants from wastewater [10]. Adsorption method has shown several advantages due to simple and smooth process, great removal performance, economically feasible, and having substantial option of adsorbent materials. Many natural materials have previously been exploited for the adsorption of contaminants

from wastewater [11]. Although, these natural adsorbents have still some limitations like low adsorption capacities and inconveniences in separation process. The scientific community declares the twenty-first century as "Pollutant Removal Age;" therefore, the exploration of novel potential adsorbents is need of the current situation.

Organic dyes, one of the most common water pollutants, have been enormously employed for the production of textiles, plastics, papers, and leather tanning [12–14]. Dyes are usually aromatic in nature and hence difficult to degrade in aquatic environments consequently imparts the adverse effects to microflora and fauna [15, 16]. Dyes also incorporate in the food chain via water sources as well as impose the toxicity on health of living things [17]. Nearly 15% of the dye is unplaced during the process of dyeing; hence, the expulsion of organic dyes from polluted water has become a considerable concern globally [18]. Graphene-based composites as adsorbents have screened extensively by the researchers for the removal of dyes [19, 20]. The exposure of nanotechnology and its implementations is considered as a breakthrough idea in the area of science and technology. Nanomaterials have attracted the significant attention due to their numerous advantageous applications in diverse fields of science. They have successfully used in antibacterial activity [21], wastewater treatment [21], anticorrosive property [22], sensing [23], imaging [24], and drug delivery system [25]. Extensive researches have been conducted for the preparation and applications of various nanomaterials to remove contaminants from wastewater. Nanomaterials like carbon nanotubes, metal oxides, and graphene have offered an innovative anticipation to the treatment of wastewater. Graphene, a one-atom-thick two-dimensional layered structure with sp^2 -hybridized carbon, is the profoundly explored compound worldwide due of its characteristic mechanical, chemical, electrical, and optical features. The oxidation of graphite results in the accumulation of oxygen functionalities such as hydroxyl, carbonyl, and epoxy groups in the graphene layer to form GO. It has a sp^2 hybridized carbon structure that is the base for 0D buckyball structures, 1D nanotubes, and 3D graphite. Graphene, due to its great theoretical surface area, has employed as an advantageous nanoadsorbent for environmental applications [26]. The generation of graphene oxide (GO), oxidized form of graphene, is occurred after incorporation of plentiful oxygen-possessing functional groups to graphene [27]. Its three-dimensional honeycomb macrostructures and monolayer of carbon having sp^2 hybridization provide the characteristics to form composites with other nanomaterials [28]. Graphene nanocomposites have been explored well for their great surface area, flexibility, large adsorption potential, and great thermal as well as electrical conductivity [29, 30]. The aforementioned characteristic factors make it an appropriate material to be designed as a nanohybrid that behaves as a photocatalyst [31–34]. 3D-GO macrostructures have also been applied for isolation of organic dye from wastewater [35]. In viewpoint of technical as well as commercial values, titanium dioxide (TiO_2) and zinc oxide (ZnO) are extensively explored photocatalysts with excellent potency for the removal of dyes [36, 37]. The current scenario of research inspires to explore the highly systematic as well as cost effective photocatalyst with composite nanomaterials for the treatment of wastewater. The literature also supported that graphene oxide-driven composites have been explored well for the degradation of anionic as well as cationic organic dyes. Therefore, in the present study, we wish to report the preparation of graphene composites and their utilities in treatment of wastewater, and the contamination caused organic dyes.

Here, iron and titanium have been chosen to synthesize nanocomposite with GO due its appropriate shape and size. It has also been expressed its utility in several areas of research such as in solar cell [38], sensor [39], and luminescent [40], electrical [41] applications. GO particles of nanorange have great specific surface area as well as sufficient numbers of active sites where the pollutant molecules actively react with photo-generated charge carriers. GO possesses hydroxyl as well as carboxyl groups [42] that exhibits super dispersibility in solvents and consequently furnishes highest possibilities for the fabrication of graphene-iron-titanium nanocomposite. Various composites have been extensively employed in treatment of environmental pollution [43]. Numerous reports are available where graphene oxide nanocomposites were exploited as a photocatalyst [44, 45], supercapacitor [46], an adsorbent [47], etc. In this report, we prepared GFT oxide nanocomposite by adopting simple and practical protocol.

2. Experimental

2.1. Materials. Graphite powder was procured from global nanotech Nagpur, sulfuric acid (98%), $NaNO_3$, $KMnO_4$, H_2O_2, HCl obtained from Merck, Mumbai. Ferrous sulphate, ferric sulphate, TiO_2 nanowires, and triple distilled water were used for overall reaction studies.

2.2. Method. First of all, GO was synthesized via oxidizing graphite applying modified Hummers' protocol [48]. Next, graphite powder (1 g) and of $NaNO_3$ (1 g) along with concentrated sulfuric acid (25 mL) were taken in an ice bath under uninterrupted stirring for 1 h followed by dropwise addition of 3 g of $KMnO_4$. Then, distilled water (60 mL) was added dropwise, the temperature was raised to 90°C, and this elevated temperature was maintained for 30 min. At last, deionized water (140 mL) was added, followed by the slow addition of H_2O_2 solution (10 mL). Then, the graphene oxide material was isolated after the process of centrifugation and this separated GO material was washed with 0.1 M HCl and deionized water until pH 7. Ultimately, the powder was dried under vacuum at 60°C for 12 h. Titanium oxide (TiO_2) nanowires and Fe_2O_3 nanoparticles were generated using the literature recommended protocols with an appropriate modification.

For preparation of TiO_2 nanowires, P25 (1.0 g) and 10 M NaOH (130 mL) were taken in a teflon-lined stainless-steel autoclave, and the temperature was maintained at 160°C for 16 h with uninterrupted stirring. Next to hydrothermal reaction, the washing of floccules was done inside the autoclave using 0.1 M HCl solution and deionized water

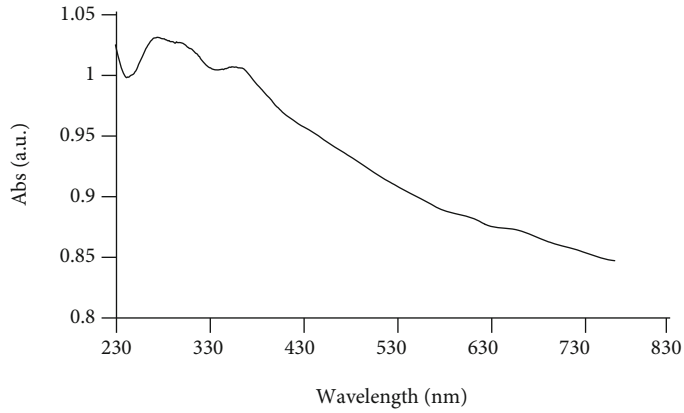

Figure 1: UV-visible spectrum of as prepared GFT.

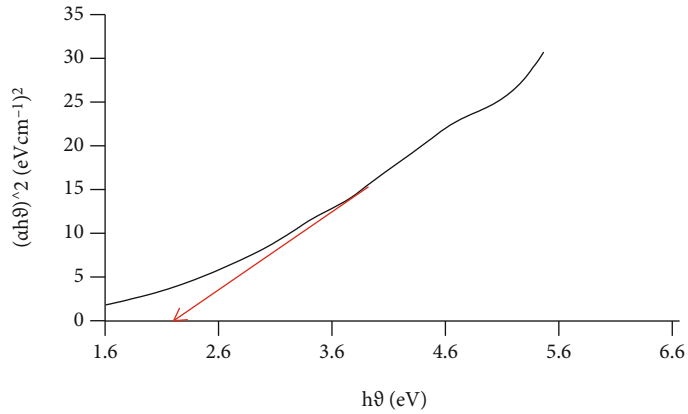

Figure 2: Band gap determination of GFT by linear extrapolation.

alternately until pH reached to approximately 7. The production of anatase-TiO_2 nanowires was completed after filtration and vacuum-drying of the materials at 60°C for 12 h then the calcination was done for 2 h at 400°C with a ramp rate of 2°C/min.

For the generation of Fe_2O_3 nanoparticles, 0.15 M $FeCl_3{\cdot}6H_2O$, isopropanol (65 mL), and NTA solution were taken in a teflon-lined autoclave and heated at 170°C for 24 h. Next to cooling, the washing of floccules was done using ethanol and deionized water alternately followed by vacuum-drying at 60°C for 12 h. Finally, calcination was done at 450°C for 3 h with a ramp rate of 2°C/min.

2.3. Synthesis of GFT. The synthesis of TiO_2 nanowire/Fe_2O_3 nanoparticle/GO sheet composite was done by adopting one-step colloid blending protocol. In a representative process, TiO_2 nanowires (100 mg), appropriate quantity of Fe_2O_3 nanoparticles and GO sheets were sonicated with each other within 150 mL deionized water for 1 h then the process was completed after overnight mixing to generate a homogeneous solution.

2.4. Characterization Study. Morphology of the prepared nanocomposites was assessed by SEM coupled using EDS (energy dispersive spectroscopy). Sample loading into adhesive copper tape was done for elementary analysis with EDS. HRTEM was employed to assess the size of the nanocomposites with shape and morphology. A UV-visible spectrophotometer (Cary win UV-Bio 50) was used to record UV-visible absorption spectra of the nanocomposites. Finally, the crystal structures of the nanocomposites were confirmed by XRD, with Cu Kα radiation operated at 40 mA in the 2θ range from 10° to 70° at a scan rate of 1°/min.

3. Results and Discussion

3.1. Characterization Studies. Figure 1 narrates UV-visible absorption spectra of prepared GFT oxide nanocomposites. Maximum wavelength (λ max) achieved at 230 nm for GO, 423 nm for TiO_2, and 407 nm for FeO. Band gap is simply calculated by the following equation.

$$1240/\text{wavelength} = h\nu. \quad (1)$$

According to equation (1) and by extraplotation of Figure 2, band gap was obtained as 2.1 eV. A band gap refers to the energy difference in semiconductors between the top of the valence band and the bottom of the conduction band using band gap energy of amorphous semiconductors using optical absorption spectra.

Figure 3 depicts XRD spectrum of GFT oxide nanomaterial. It assists to know out crystal size, basic crystal features,

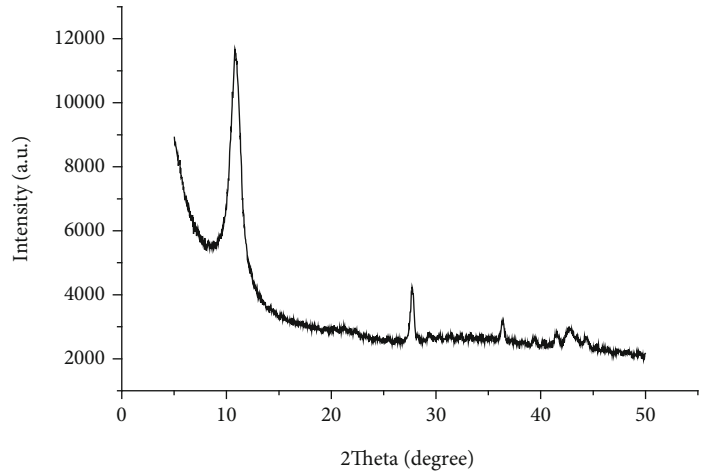

Figure 3: XRD spectrum of as synthesized GFT oxide nanocomposite.

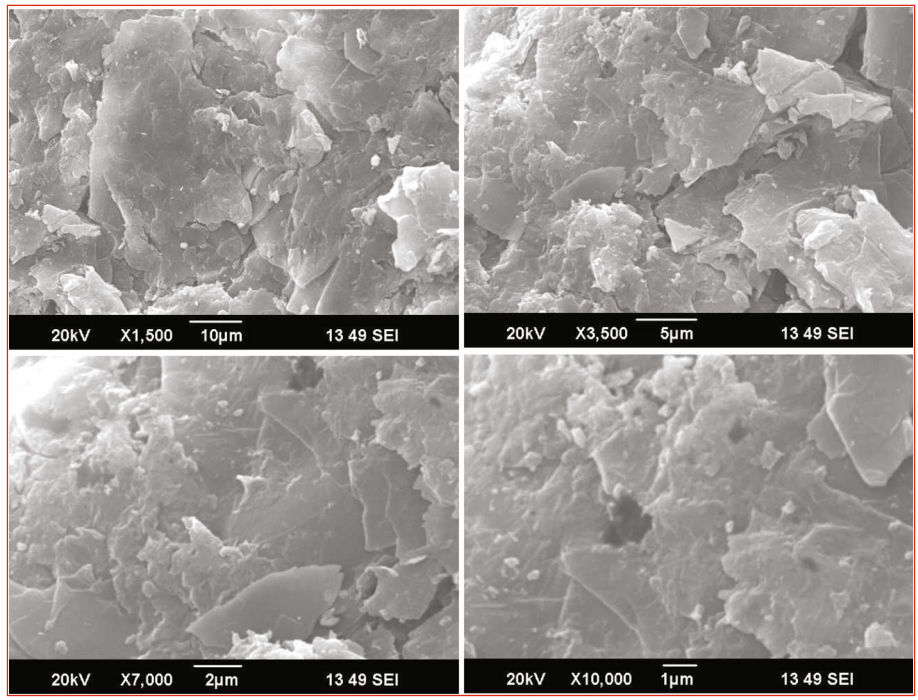

Figure 4: SEM image of as synthesized GFT nanocomposite with different magnification.

lattice, plane, interlayer spacing, microstrain, etc. A sharp and intense peak with 2θ at 10.86°, 27.79°, and 36.46°, respectively. Peak at 10.86° indicates presence of graphene oxide with 001 plane, while rest other peaks 27.79° and 36.46° resemble to iron oxide and titanium oxide, respectively. Presence of most intense peak reveals maximum presence of GO in nanocomposite.

SEM images as shown in Figure 4 reveals rough surface of as prepared GFT oxide nanocomposite. It indicates porous structure with various active sites, which made it more suitable for catalysis.

EDX spectrum of confirms the presence of C, Fe, O, and Ti atoms in prepared GFT oxide nanocomposite. It is clearly seen in inset table (Figure 5) and percentage of GO is greater than Ti and Fe.

The HRTEM images of various magnification from 0.5 μm to 20 nm (Figures 6(a)–6(e)) clearly show that TiO_2 nanorods and iron oxide nanoparticles are spread over the graphene sheets. SAED pattern (Figure 6(f)) of as synthesized GFT oxide nanocomposite shows crystalline nature of prepared material, and it is quite resembled to XRD data.

Figure 7 shows TGA spectrum of GFT oxide. At lower temperature, there is no significant changes have been observed in nanocomposite. The degradation occurs after 200°C, this can be attributed to the intercalation/exfoliation, from 200–500°C, there is little loss is seen and after that composite is almost stable at higher temperature.

Figure 8 shows FT-IR spectrum of GFT oxide nanocomposite demonstrates a broad band at 3416.11 cm^{-1} and the band at 1627.69 cm^{-1} appears due to the surface-adsorbed

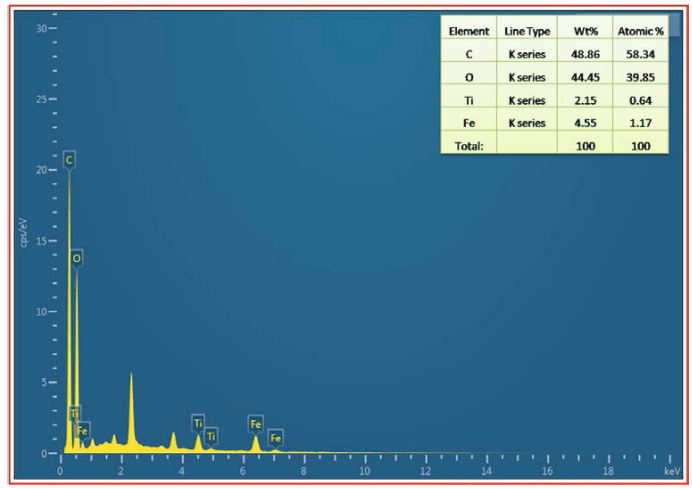

Figure 5: EDX spectrum of as synthesized GFT nanocomposite.

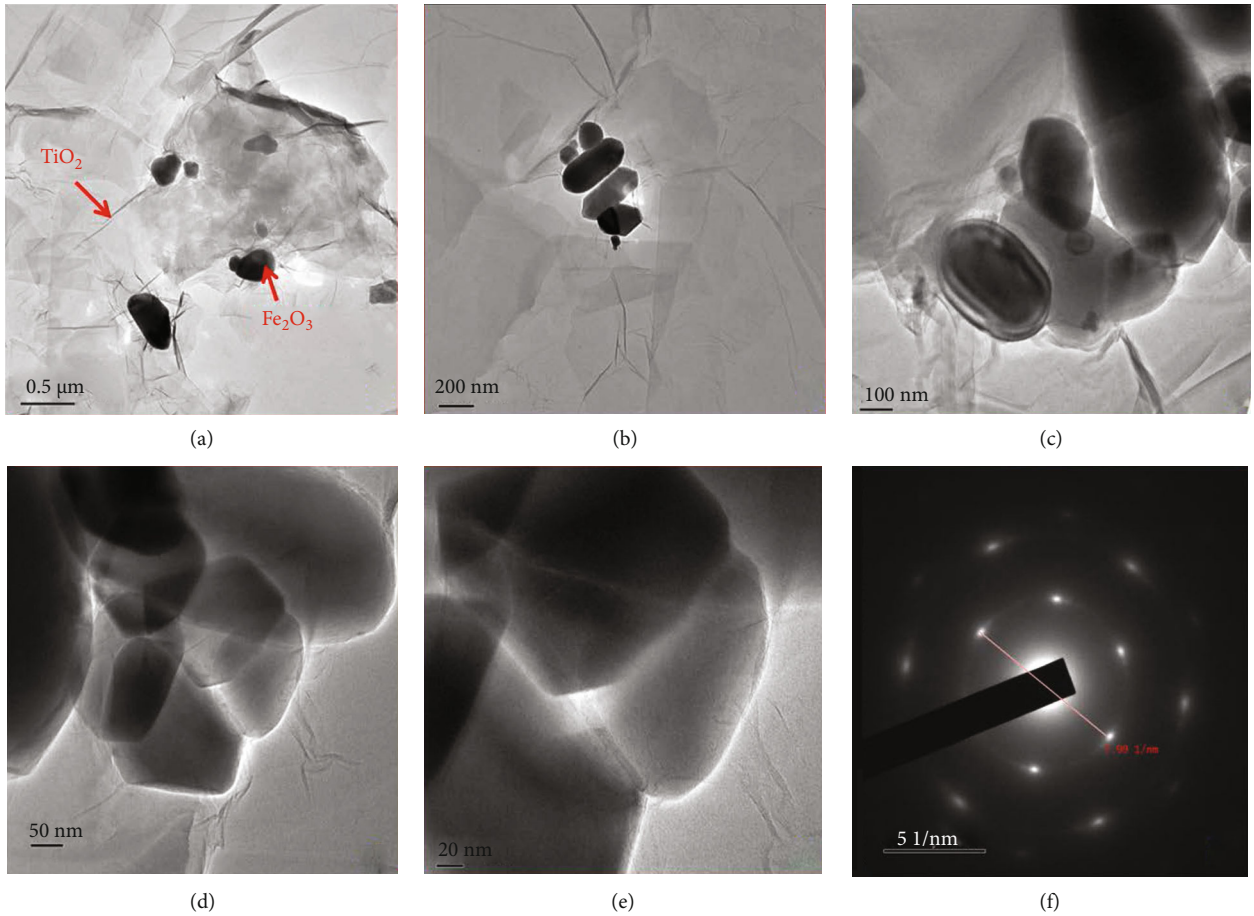

(a) (b) (c)

(d) (e) (f)

Figure 6: HRTEM image of as synthesized GFT oxide nanomaterial, (a)–(e) 0.5 μm to 20 nm, (f) crystal fringes obtained from SAED pattern.

water, and this infers the presence of –OH functional groups. Comparatively, the band at 2854.10-3172.82 cm^{-1} denoting the presence of H-bonding in the produced nanocomposite. Reduction of hydrazine results in the incorporation of nitrogen moieties onto graphene, the OH groups available on the surface of titanium could generate H-bonds with the NH groups present on the graphene sheets to produce the composite. Moreover, extra band at 1122.81 cm^{-1} is appeared in the spectrum observed for GFT oxide nanocomposite, and this can be indicated to Ti-O-C-Fe vibrations. Because hydrazine is unable to execute a full reduction of graphene oxide, the Ti-O-C bond may

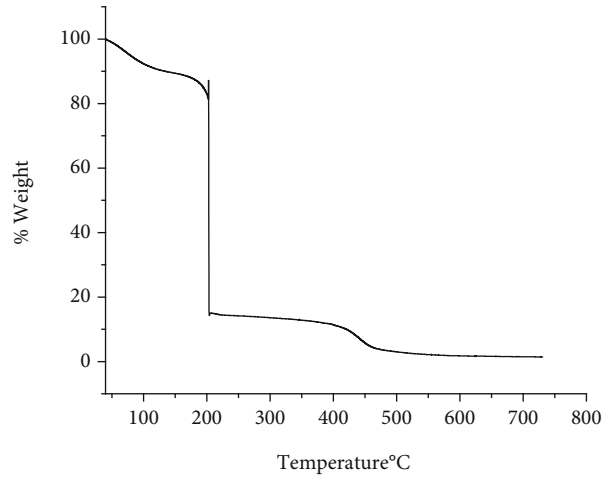

Figure 7: TGA spectrum of as synthesized GFT oxide nanocomposite.

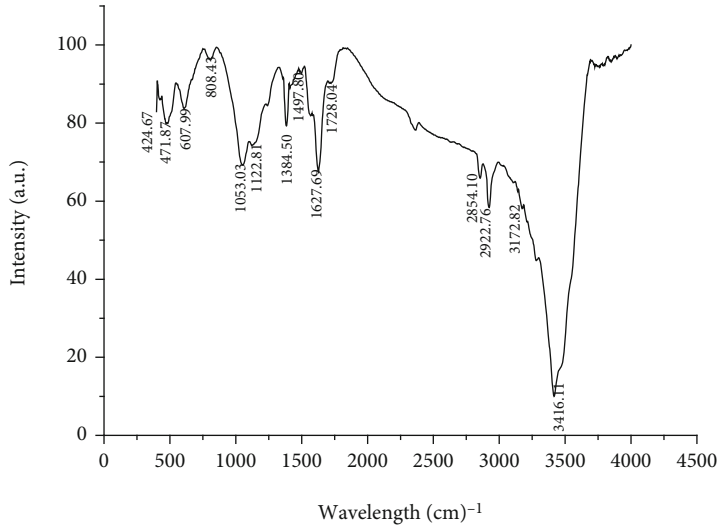

Figure 8: FT-IR spectrum of as synthesized GFT oxide nanocomposite.

be generated when OH groups available on TiO_2 react with residual OH groups present on the graphene sheets in removing water. Table 1 summarizes all FTIR results.

3.2. Degradation of Dye by Fenton's Process. The degradation/abatement studies provide an information for the efficiency and mechanism of a process. Present work done at the optimal conditions for AM dye solution. Figure 9 shows the abatement of AM at different oxidation conditions, i.e., H_2O_2 alone, GFT alone, and GFT + H_2O_2 (heterogeneous Fenton) by decrease in absorbance at 510 nm with the passage to time. Figure 9 shows that H_2O_2 and GFT alone are unable to effectively remove the AM dye from aqueous solution. With the heterogeneous Fenton process (GFT + H_2O_2), maximum removal is achieved in 240 minutes.

3.3. Mechanism of Fenton Degradation. Fenton process is regarded as one of the most fruitful progressive catalytic processes for the removal of many toxic organic pollutants from wastewater. The reaction between aqueous ferrous ions and

Table 1: FTIR spectrum of all functional groups present in GFT nanocomposites.

Band (cm^{-1})	Functional group
424.67	Graphene oxide
471.87	Iron oxide
607.99	Titanium oxide
1053.03	Alcoxy C-O
1122.81	Ti-O-C-Fe nanocomposite
1384.50	Phenolic C-O-H
1497.80	Epoxy C-O
1627.69	Surface adsorbed water
1728.04	Carboxyl C=O
2854.10	H bonding
2922.76	H bonding
3172.82	H bonding
3416.11	Surface adsorbed water

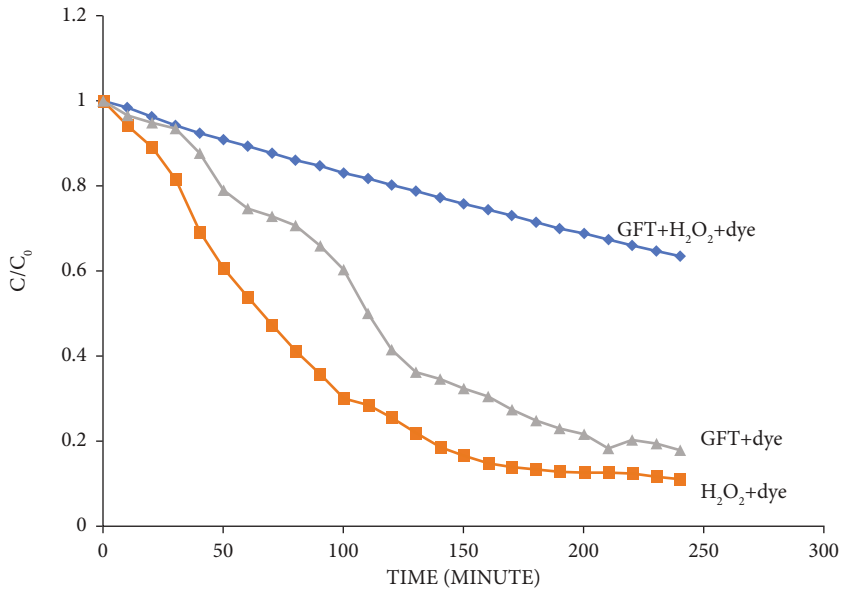

Figure 9: Degradation of AM at different oxidation conditions (H_2O_2 and GFT alone and H_2O_2 + GFT). Reaction conditions: [AM] = 140 mg/L, [H_2O_2] = 20mM, [GFT] = 0.2 g/L at pH 8.

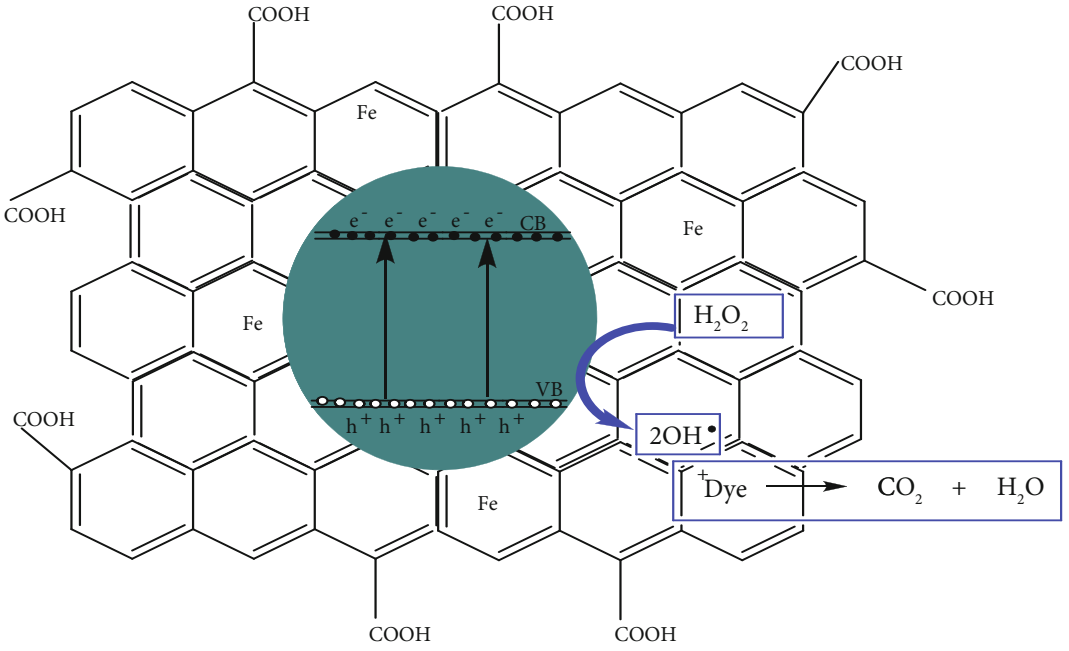

Figure 10: Plausible mechanism for degradation of dye by heterogeneous Fenton reaction.

hydrogen peroxide (H_2O_2) generates hydroxyl radical (·OH), and it can degrade refractory as well as hazardous organic pollutants in wastewater [49]. Hence, scientific community is paying more attention on Fenton processes for removal of contaminants from wastewater. Recently, various modifications have been executed on homogeneous and heterogeneous Fenton processes to attain maximum efficiency [50–52]. It has been observed that the degradation process is significantly enhanced after introduction of metal oxide as a heterogeneous catalyst [53–57]. A considerable advantage of heterogeneous Fenton reaction is its applicability over a broad range of pH to destroy organic pollutants present in wastewater.

On the basis of literature reports and observations, herein, we proposed a plausible mechanism for Fenton process (Figure 10). Central carbon atom of cationic dye acts as an electrophile. In Fenton process, the generated radical acts as a nucleophile. This nucleophile attacks the electrophile to break it into small molecules. Several radicals are reported in Fenton's process, but $^{\bullet}OH$ mostly destroys the quinone moiety of dye very efficiently. GFT generates a hole as well as an electron after irradiation of sunlight. Photoelectron jumps to

the conduction band consequently a hole is generated in the valance band. Next, the generated hole reacts with an aqueous reaction mixture to furnish hydroxyl radicals. Then, after the reaction of electrons from the conduction band with dissolved oxygen, superoxide radical anion ($\bullet O_2^-$) is generated. As per the oxidation potential of superoxide radical anion and hydroxyl radical, hydroxyl radical is more responsible and hence the dye is decolorized efficiently (Equation (2)–(7)).

$$(\text{Nanocomposites as catalyst}) + H_2O_2 \longrightarrow (\text{CB})\, e^- + (\text{VB})\, h^+, \quad (2)$$

$$(\text{CB})\, e^- + O_2 \longrightarrow O_2^{\cdot\circ-}\,(\text{radical}), \quad (3)$$

$$O_2^{\cdot-} + H_2O \longrightarrow HO_2^{\cdot} + OH^-, \quad (4)$$

$$(\text{VB})\, h^+ + OH^- \longrightarrow OH^{\cdot}\,(\text{adsorbed}), \quad (5)$$

$$(\text{VB})\, h^+ + HO_2^{\cdot} \longrightarrow {}^{\circ}OH^{\cdot} + H^+, \quad (6)$$

Ultimately, oxidation of dye molecules yields water and CO_2.

$${}^{\circ}OH^{\cdot} + O_2 + \text{Dye molecules} \longrightarrow CO_2 + H_2O, \quad (7)$$

4. Conclusion

In this study, GFT oxide nanocomposite has been synthesized as well as characterized successfully. XRD and SAED patterns confirm its crystalline behavior. Rod-like shape of titanium oxide and oval shape iron oxide nanomaterial spread on GO sheets is clearly seen in SEM images. Stability of prepared GFT oxide nanocomposite was determined by TGA and confirms its stability at higher temperature. As per environmental concerns, the synthesized nanocomposite was exploited as catalyst for removal of organic dye in Fenton process and the results showed that the catalytic efficacy of synthesized nanocomposite was found to be adequate.

Data Availability

Authors can also make data available on request through a data access committee, institutional review board, or the authors themselves. Corresponding author who should be contacted to request the data.

Conflicts of Interest

All authors declare that we have no conflict of interest.

Acknowledgments

This study was supported by Princess Nourah Bint Abdulrahman University Researchers Supporting Project number (PNURSP2022R26), Princess Nourah Bint Abdulrahman University, Riyadh, Saudi Arabia.

References

[1] C. M. B. Araujo, R. B. Assis Filho, A. M. S. Baptisttella et al., "Recent developments in photocatalytic water treatment technology: a review," *Water Research*, vol. 44, no. 10, pp. 2997–3027, 2010.

[2] G. M. Zeng, X. Li, J. H. Huang et al., "Micellar-enhanced ultrafiltration of cadmium and methylene blue in synthetic wastewater using SDS," *Journal of Hazardous Materials*, vol. 185, no. 2-3, pp. 1304–1310, 2011.

[3] G. Zeng, M. Chen, and Z. Zeng, "Shale gas: surface water also at risk," *Nature*, vol. 499, no. 7457, article 154, 2013.

[4] P. Xu, G. M. Zeng, D. L. Huang et al., "Adsorption of Pb(II) by iron oxide nanoparticles immobilized Phanerochaete chrysosporium : equilibrium, kinetic, thermodynamic and mechanisms analysis," *Chemical Engineering Journal*, vol. 203, pp. 423–431, 2012.

[5] H. Chen, G. Dai, J. Zhao, A. Zhong, J. Wu, and H. Yan, "Removal of copper(II) ions by a biosorbent–cinnamomum camphora leaves powder," *Journal of Hazardous Materials*, vol. 177, no. 1-3, pp. 228–236, 2010.

[6] M. Hua, S. Zhang, B. Pan, W. Zhang, L. Lv, and Q. Zhang, "Heavy metal removal from water/wastewater by nanosized metal oxides: a review," *Journal of Hazardous Materials*, vol. 211-212, pp. 317–331, 2012.

[7] F. Fu and Q. Wang, "Removal of heavy metal ions from wastewaters: a review," *Journal of Environmental Management*, vol. 92, no. 3, pp. 407–418, 2011.

[8] Y. H. Wang, S. H. Lin, and R. S. Juang, "Removal of heavy metal ions from aqueous solutions using various low-cost adsorbents," *Journal of Hazardous Materials*, vol. 102, no. 2-3, pp. 291–302, 2003.

[9] I. Ali, "New generation adsorbents for water treatment," *Chemical Reviews*, vol. 112, no. 10, pp. 5073–5091, 2012.

[10] C. M. Zvinowanda, J. O. Okonkwo, P. N. Shabalala, and N. M. Agyei, "A novel adsorbent for heavy metal remediation in aqueous environments," *International journal of Environmental Science and Technology*, vol. 6, no. 3, pp. 425–434, 2009.

[11] S. J. T. Pollard, G. D. Fowler, C. J. Sollars, and R. Perry, "Low-cost adsorbents for waste and wastewater treatment: a review," *Science of the Total Environment*, vol. 116, no. 1-2, pp. 31–52, 1992.

[12] E. Brillas and C. A. Martínez-Huitle, "Decontamination of wastewaters containing synthetic organic dyes by electrochemical methods. An updated review," *Applied Catalysis B: Environmental*, vol. 166-167, pp. 603–643, 2015.

[13] S. Shukla and M. A. Oturan, "Dye removal using electrochemistry and semiconductor oxide nanotubes," *Environmental Chemistry Letters*, vol. 13, no. 2, pp. 157–172, 2015.

[14] H. D. Lee, J. O. Kim, and J. W. Chung, "Degradation of methyl orange by pulsed corona discharge process in water," *Desalination and Water Treatment*, vol. 53, no. 10, pp. 2767–2773, 2015.

[15] G. F. O. Nascimento, G. R. B. Costa, M. N. Carvalho, M. G. Ghislandi, and M. A. da Motta Sobrinho, "Systematic study of graphene oxide production using factorial design techniques and its application to the adsorptive removal of methylene blue dye in aqueous medium," *Materials Research Express*, vol. 5, no. 6, article 065042, 2018.

[16] T. Ma, P. R. Chang, P. Zheng, F. Zhao, and X. Ma, "Fabrication of ultra-light graphene-based gels and their adsorption of

methylene blue," *Chemical Engineering Journal*, vol. 240, pp. 595–600, 2014.

[17] K. Mohanty, J. T. Naidu, B. C. Meikap, and M. N. Biswas, "Removal of crystal violet from wastewater by activated carbons prepared from rice husk," *Industrial & Engineering Chemistry Research*, vol. 45, no. 14, pp. 5165–5171, 2006.

[18] A. Houas, H. Lachheb, M. Ksibi, E. Elaloui, C. Guillard, and J. M. Herrmann, "Photocatalytic degradation pathway of methylene blue in water," *Applied Catalysis B: Environmental*, vol. 31, no. 2, pp. 145–157, 2001.

[19] F. Liu, S. Chung, G. Oh, and T. S. Seo, "Three-dimensional graphene oxide nanostructure for fast and efficient water-soluble dye removal," *ACS Applied Materials & Interfaces*, vol. 4, no. 2, pp. 922–927, 2012.

[20] G. K. Ramesha, A. V. Kumara, H. B. Muralidhara, and S. Sampath, "Graphene and graphene oxide as effective adsorbents toward anionic and cationic dyes," *Journal of Colloid and Interface Science*, vol. 361, no. 1, pp. 270–277, 2011.

[21] H. Lu, J. Wang, M. Stoller, T. Wang, Y. Bao, and H. Hao, "An overview of nanomaterials for water and wastewater treatment," *Advances in Materials Science and Engineering*, vol. 2016, 10 pages, 2016.

[22] X. Shi, T. A. Nguyen, Z. Suo, Y. Liu, and R. Avci, "Effect of nanoparticles on the anticorrosion and mechanical properties of epoxy coating," *Surface and Coating Technology*, vol. 204, no. 3, pp. 237–245, 2009.

[23] X. Luo, A. Morrin, A. J. Killard, and M. R. Smyth, "Application of nanoparticles in electrochemical sensors and biosensors," *Electroanalysis*, vol. 18, no. 4, pp. 319–326, 2006.

[24] B. Li, J. Tang, W. Chen et al., "Novel theranostic nanoplatform for complete mice tumor elimination via MR imaging-guided acid-enhanced photothermo-/chemo-therapy," *Biomaterials*, vol. 177, pp. 40–51, 2018.

[25] A. Z. Wilczewska, K. Niemirowicz, K. H. Markiewicz, and H. Car, "Nanoparticles as drug delivery systems," *Pharmacological Reports*, vol. 64, no. 5, pp. 1020–1037, 2012.

[26] K. S. Novoselov, V. I. Fal'ko, L. Colombo, P. R. Gellert, M. G. Schwab, and K. Kim, "A roadmap for graphene," *Nature*, vol. 490, no. 7419, pp. 192–200, 2012.

[27] S. Virendra, J. Daeha, L. Zhai, S. Das, and I. K. Sudipta, "Graphene based materials: past, present and future," *Progress in Materials Science*, vol. 56, no. 8, pp. 1178–1271, 2011.

[28] G. Eda, G. Fanchini, and M. Chhowalla, "Large-area ultrathin films of reduced graphene oxide as a transparent and flexible electronic material," *Nature Nanotechnology*, vol. 3, no. 5, pp. 270–274, 2008.

[29] A. K. Geim and K. S. Novoselov, "The rise of graphene," *Nature Materials*, vol. 6, no. 3, pp. 183–191, 2007.

[30] M. Chandel, D. Moitra, P. Makkar, H. Sinha, H. S. Hora, and N. N. Ghosh, "Synthesis of multifunctional CuFe2O4-reduced graphene oxide nanocomposite: an efficient magnetically separable catalyst as well as high performance supercapacitor and first-principles calculations of its electronic structures," *RSC Advances*, vol. 8, no. 49, pp. 27725–27739, 2018.

[31] M. Bagherzadeh and R. Kaveh, "New magnetically recyclable reduced graphene oxide rGO/MFe2O4(M= Ca, Mg)/Ag3PO4-nanocomposites with remarkably enhanced visible-light photocatalytic activity and stability," *Photochemistry and Photobiology*, vol. 94, no. 6, pp. 1210–1224, 2018.

[32] C. Basheer, "Application of titanium dioxide-graphene composite material for photocatalytic degradation of alkylphenols," *Journal of Chemistry*, vol. 2013, 10 pages, 2013.

[33] G. Rao, Q. Zhang, H. Zhao, J. Chen, and Y. Li, "Novel titanium dioxide/iron (III) oxide/graphene oxide photocatalytic membrane for enhanced humic acid removal from water," *Chemical Engineering Journal*, vol. 302, pp. 633–640, 2016.

[34] B. Mandal, P. Sarkar, and C. Chakravarty, "Porous graphene-fullerene nanocomposites: a new composite for solar cell and optoelectronic application," *Journal of Physical Chemistry C*, vol. 122, no. 28, pp. 15835–15842, 2018.

[35] H. Kim, S. O. Kang, S. Park, and H. S. Park, "Adsorption isotherms and kinetics of cationic and anionic dyes on three-dimensional reduced graphene oxide macrostructure," *Journal of Industrial and Engineering Chemistry*, vol. 21, pp. 1191–1196, 2015.

[36] R. Wahab, S. K. Tripathy, H. S. Shin et al., "Photocatalytic oxidation of acetaldehyde with ZnO-quantum dots," *Chemical Engineering Journal*, vol. 226, pp. 154–160, 2013.

[37] E. S. Elmolla and M. Chaudhuri, "Photocatalytic degradation of amoxicillin, ampicillin and cloxacillin antibiotics in aqueous solution using UV/TiO_2 and $UV/H_2O_2/TiO_2$ photocatalysis," *Desalination*, vol. 252, no. 1-3, pp. 46–52, 2010.

[38] K. L. Chopra and S. R. Das, *Thin Film Solar Cells*, Plenum, NewYork, 1983.

[39] B. B. Rao, "Zinc oxide ceramic semi-conductor gas sensor for ethanol vapour," *Materials Chemistry and Physics*, vol. 64, no. 1, pp. 62–65, 2000.

[40] I. M. Povey, V. Z. Zubialevich, M. Schmidt, J. Kegel, and M. E. Pemble, "Effect of surface and defect chemistry on the photocatalytic properties of intentionally defect-rich ZnO nanorod arrays," *ACS Applied Materials & Interfaces*, vol. 10, no. 21, pp. 17994–18004, 2018.

[41] S. Hingorani, V. Pillai, P. Kumar, M. S. Multani, and D. O. Shah, "Microemulsion mediated synthesis of zinc-oxide nanoparticles for varistor studies," *Materials Research Bulletin*, vol. 28, no. 12, pp. 1303–1310, 1993.

[42] B. Jain, A. Hashmi, S. Sanwaria, A. K. Singh, M. A. B. H. Susan, and S. A. C. Carabineiro, "Catalytic properties of graphene oxide synthesized by a "Green" process for efficient abatement of Auramine-O cationic dye," *Analytical Chemistry Letters*, vol. 10, no. 1, pp. 21–32, 2020.

[43] G. Manjari, S. Saran, S. P. Devipriya, and A. V. B. Rao, "Novel synthesis of Cu@ZnO and Ag@ZnO nanocomposite via green method: a comparative study for ultra-rapid catalytic and recyclable effects," *Catalysis Letters*, vol. 148, no. 8, pp. 2561–2571, 2018.

[44] S. P. Lonkar, V. Pillai, and A. Abdala, "Solvent free synthesis of ZnO graphene nanocomposites with superior photocatalytic activity," *Applied Surface Science*, vol. 465, pp. 1107–1113, 2019.

[45] R. Atchudan, T. N. J. I. Edison, S. Perumal, D. Karthikeyan, and Y. R. Lee, "Facile synthesis of zinc oxide nanoparticles decorated graphene oxide composite via simple solvothermal route and their photocatalytic activity on methylene blue degradation," *Journal of Photochemistry and Photobiology B: Biology*, vol. 162, pp. 500–510, 2016.

[46] I. Y. Y. Bu and R. Huang, "One-pot synthesis of ZnO/reduced graphene oxide nanocomposite for supercapacitor applications," *Materials Science in Semiconductor Processing*, vol. 31, pp. 131–138, 2015.

[47] J. Wang, T. Tsuzuki, X. Hou, L. Sun, and X. Wang, "Reduced graphene oxide/ZnO composite: reusable adsorbent for pollutant management," *ACS Energy Letters*, vol. 4, no. 6, pp. 3084–3090, 2012.

[48] N. I. Zaaba, K. L. Foo, U. Hashim, S. J. Tan, W. W. Liu, and C. H. Voon, "Synthesis of graphene oxide using modified hummers method: solvent influence," *Procedia Engineering*, vol. 184, pp. 469–477, 2017.

[49] M. S. Lucas, A. A. Dias, A. Sampaio, C. Amaral, and J. A. Peres, "Degradation of a textile reactive Azo dye by a combined chemical-biological process: Fenton's reagent-yeast," *Water Research*, vol. 41, no. 5, pp. 1103–1109, 2007.

[50] I. Michael, E. Hapeshi, C. Michael et al., "Solar photo-Fenton process on the abatement of antibiotics at a pilot scale: degradation kinetics, ecotoxicity and phytotoxicity assessment and removal of antibiotic resistant enterococci," *Water Research*, vol. 46, no. 17, pp. 5621–5634, 2012.

[51] I. Michael, E. Hapeshi, J. Acena et al., "Light-induced catalytic transformation of ofloxacin by solar Fenton in various water matrices at a pilot plant: mineralization and characterization of major intermediate products," *Science of the Total Environment*, vol. 461-462, pp. 39–48, 2013.

[52] A. Mirzaei, Z. Chen, F. Haghighat, and L. Yerushalmi, "Removal of pharmaceuticals from water by homo/heterogonous Fenton-type processes - a review," *Chemosphere*, vol. 174, pp. 665–688, 2017.

[53] O. García-Rodríguez, J. A. Bañuelos, L. A. Godínez et al., "Iron supported on ion exchange resin as source of iron for Fenton reagent: a heterogeneous or a homogeneous Fenton reagent generation?," *International Journal of Chemical Reactor Engineering*, vol. 15, no. 5, 2017.

[54] Z. Diao, X. Xu, D. Jiang et al., "Enhanced catalytic degradation of ciprofloxacin with FeS_2/SiO_2 microspheres as heterogeneous Fenton catalyst: kinetics, reaction pathways and mechanism," *Journal of Hazardous Materials*, vol. 327, pp. 108–115, 2017.

[55] H. Narayani, H. Arayapurath, and S. Shukla, "Using Fenton-reaction as a novel approach to enhance the photocatalytic activity of TiO2-γ-Fe2O3 magnetic photocatalyst undergoing photo-dissolution process without silica interlayer," *Catalysis Letters*, vol. 143, no. 8, pp. 807–816, 2013.

[56] E. V. Parkhomchuk, J. Gracia-Aguilar, K. A. Sashkina et al., "ParmonVN(2018) Ferrosilicate-based heterogeneous Fenton catalysts: influence of crystallinity, porosity and iron speciation," *Catalysis Letters*, vol. 148, no. 10, pp. 3134–3146, 2018.

[57] P. Bouras and P. Lianos, "Synergy effect in the combined photodegradation of an azo dye by titanium dioxide photocatalysis and photo-Fenton oxidation," *Catalysis Letters*, vol. 123, no. 3-4, pp. 220–225, 2008.